

PACS numbers: 42.55.Wd; 42.65.–k; 42.81.–i
DOI: 10.1070/QE2015v045n07ABEH015593

Broadband supercontinuum generation in a telecommunication fibre pumped by a nanosecond Tm, Ho : YVO_4 laser

Zhou Ren-Lai, Ren Jian-Cun, Lou Shu-Li, Ju You-Lun, Wang Yue-Zhu

Abstract. **Broadband supercontinuum (SC) generation in a telecommunication fibre [8/125-μm single mode fibre (SMF) and 50/125-μm multimode fibre (MMF)] directly pumped by a nanosecond *Q*-switched Tm, Ho : YVO_4 laser is demonstrated. At a 7-kHz pulse repetition frequency (PRF), an output average power of 0.53 W in the 1.95 – 2.5-μm spectral band and 3.51 W in the 1.9 – 2.6-μm spectral band are achieved in SMF and MMF, respectively (the corresponding optic-to-optic conversion efficiencies are 34.6 % and 73.7 %). The output spectra have extremely high flat segments in the range 2070 – 2390 nm and 2070 – 2475 nm with negligible intensity variation (less than 2 %). The SC average power is scalable from 2.1 to 4.2 W by increasing the PRF from 5 to 15 kHz, while maintaining pump power. Compared with the input pump pulse, the output SC pulse width is broadened, and no split is found. The stability of the output SC power has been monitored for a week and the fluctuations being less than 6 %.**

Keywords: *supercontinuum generation, telecommunication fibre, Tm, Ho : YVO_4 laser, nanosecond pulse.*

1. Introduction

Supercontinuum (SC) generation in optical fibres has been the subject of extensive research in recent years due to the great fundamental interest and its potential applications in atmosphere analysis, spectroscopy, free-space communications, biology and medicine [1 – 3], especially in the mid-infrared (mid-IR) spectral region. With the recent development of various special optical fibres, including microstructure fibres (MFs) [4 – 6], fibre tapers [7], highly nonlinear fibres (HNLFs) [8, 9], fluoride fibres [10 – 12], tellurite fibres [13] and chalcogenide fibres [14], a broadband SC source can be efficiently generated by pumping with high power pulsed lasers (femtosecond, picosecond and nanosecond pulses) or even with cw lasers.

Many different experiment configurations for SC generation have been reported in recent years in the literature, mode-locked lasers or short pulse amplifiers being always used as pump sources, which make it possible to reach a high peak power. However, limited by pump pulse energy and the fibre core size, it is difficult to obtain SC with a high output energy, such as an up to 25.7-W SC based on a power scalable thulium-doped fibre amplifier (TDFA). SC laser spanning from ~2 to 2.5 μm was recently demonstrated by Alexander et. al. [15], but the PRF was ~1.1 MHz, and the pulse energy was only ~23.4 μJ. Additionally, due to the high nonlinearity and material dispersion in special optical fibres, the output time-domain SC pulse is always broken up into a series of shorter pulses, and the pulse energy is dispersed. Furthermore, most researcher study SC generation in all kinds of special fibres, less attention has been paid to SC generation in the mid-IR range with use of a cheap and widely commercially available telecommunication fibre pumped by > 2000 nm nanosecond pulses of solid-state lasers.

In this paper, we demonstrate broadband SC laser generation in a conventional telecommunication fibre pumped by a nanosecond *Q*-switched Tm, Ho : YVO_4 laser. Previously, the mid-IR SC laser generation in SMF or MMF relied on pumping by a ~1550-nm pulsed fibre laser or amplifier [16 – 20] with the maximal output power being only 1.1 W at $\lambda > 1650$ nm and PRF of 200 kHz [18]. The maximal output power of a Tm, Ho : YVO_4 laser emitting at 2.054 μm is ~9.2 W at 7 kHz, and the minimal pulse width is ~25 ns. The output wavelength of the SC laser exceeds 1900 nm, and the maximal achieved average power and pulse energy are 4.2 W and ~0.5 mJ, respectively.

2. Experimental setup

Figure 1 shows the experimental setup of SC generation in telecommunication fibre. The fibre coupled laser diodes with a maximal output power of 35 W was used as a pump source, and the emitting wavelength was in the range of 798 – 802 nm. The diameter of the output fibre was 400 μm, and the numerical aperture (NA) was 0.22. The Tm, Ho : YVO_4 laser resonator geometry was plano-concave, and the physical cavity length of the resonator was about 300 mm. A flat mirror (M7) had a 40 % transmission in the range of 1.9 – 2.2 μm. The focal length of the coupling lens (L1) was 25 mm. Lenses (L2 and L3) were mode matching lenses with a focal length of 50 mm. A dichromatic mirror (M1) had a partial reflectivity of 50% at ~800 nm, and the reflectivity *R* of dichromatic mirrors (M2, M3 and M4) was ⩾ 99.5 % at $\lambda \sim 800$ nm. The Tm, Ho : YVO_4 bonding crystal for the experiment was *a*-cut with dimensions of 3×3×8 mm, and the ion dopant concentrations were 4 at % Tm^{3+}, 0.4 at % Ho^{3+}. Both end faces of the crystal were anti-reflection (AR) coated for the laser wavelengths around 2 μm and the pump wavelength around 800 nm. The laser crystal was placed in the vicinity of lens focus (L2 and L3), and the

Zhou Ren-Lai, Ren Jian-Cun, Lou Shu-Li Department of control engineering, Naval Aeronautical & Astronautical University, Yantai 264001, China; e-mail: zrlhit@126.com;
Ju You-Lun, Wang Yue-Zhu National Key Laboratory of Tunable Laser Technology, Harbin Institute of Technology, No. 2, Yi kuang Street, Nan gang District, Harbin 150080, China

Received 22 June 2014; revision received 20 September 2014
Kvantovaya Elektronika **45** (7) 621 – 624 (2015)
Submitted in English

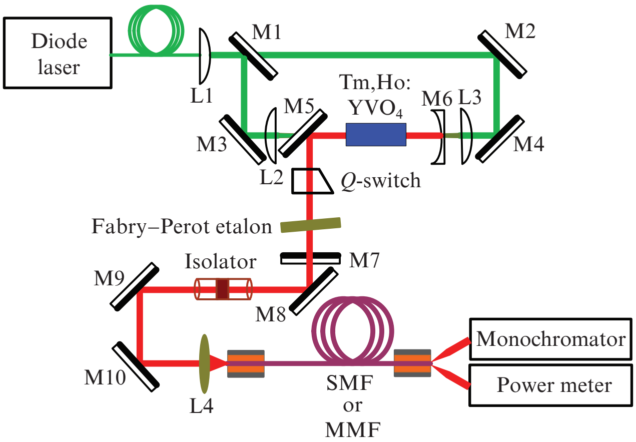

Figure 1. Experimental setup of SC generation in telecommunication fibre.

measured confocal spot of 800-nm laser pump, inside of the laser crystal surface, was approximately 0.75 mm.

The laser crystal was wrapped in indium foil, clamped in a copper heat-sink and placed in a dewar, which was used as the liquid nitrogen reservoir. Q-switching was achieved with a 46-mm-long fused silica acousto-optical Q-switch. Its maximum RF power was 50 W and the repetition rate could be tuned continuously from 1 Hz to 100 kHz. To achieve a single wavelength operation, a 0.1-mm-thick Fabry–Perot etalon was also inserted into the optical path, and the 2.054 μm output laser wavelength was selected. Dichromatic mirrors (M8, M9 and M10) had $R \geqslant 97\%$ at 2.05 μm and a transmission coefficient $T \geqslant 90\%$ at 800 nm. The telecommunication fibre used in experiment had a graded refractive index profile and the core/clad diameter of 8/125 μm or 50/125 μm. The double ends of fibre were perpendicular cleaved and clamped in a copper heat sink. The output 2.054 μm laser was coupled into fibre core by a focusing lens (L4) (f = 9 mm), and the measured coupling efficiency was ~29% (SMF) or ~70% (MMF). In order to prevent the Tm, Ho : YVO_4 pump laser from being influenced by the fibre end feedback and the nonlinear laser (SBS), an optical isolator was placed into the pump path.

3. Results and discussion

Spectral measurements were acquired using a monochromator (300 mm focal length, 600 lines mm^{-1} grating blazed at 2.0 μm), an InGaAs detector (rise/fall time < 23 ns) covering the spectral band of 1.2–2.6 μm, and a SR830 lock-in amplifier which was used to extract the signal. The spectrum evolution of the laser SC, generated from the SMF and MMF, is shown in Fig. 2. The SMF or MMF used in the experiment had a length of 15 m. Note that the spectral width is set by the injected pump power. However, the injected pump powers were limited by the damage threshold of fibre ends, and the maximal injected pump powers of SMF and MMF in the experiment were 1.53 and 4.76 W. In the case of SMF, the SC spectrum extends from ~1950 to ~2500 nm at 0.53 W output (Fig. 2a), the shape of the spectrum being virtually flat in the wavelength interval of 2070–2390 nm with a negligible intensity variation (less than 2%). By replacing the SMF with a MMF, the SC spectrum extends from ~1920 to ~2600 nm at 3.51 W output (Fig. 2b), and the flat output spectrum is

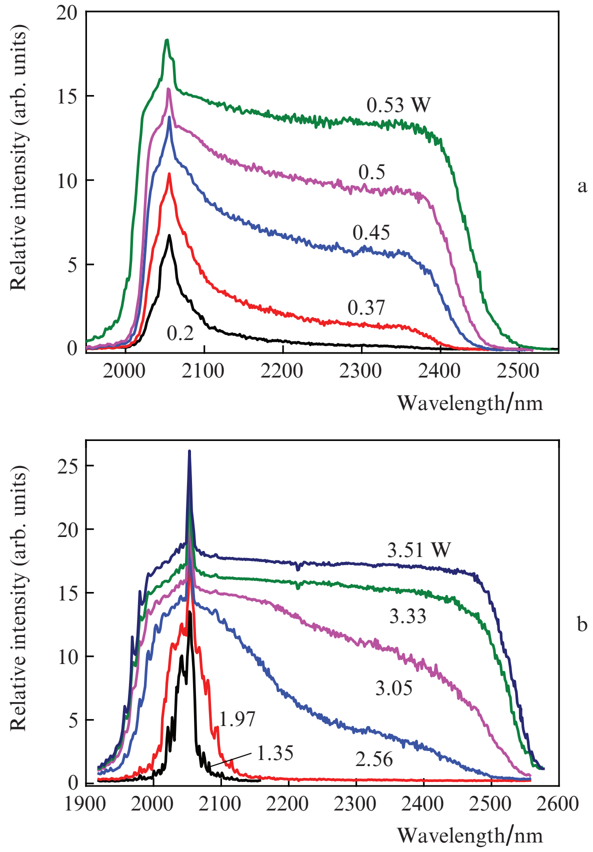

Figure 2. SC emission spectrum generation in (a) SMF and (b) MMF at different SC output powers.

observed in the wavelength interval of 2070–2475 nm. However, of particular importance is the fact that the extremely stable output spectrum is a result of averaging over many laser pulses, and the main reason can be attributed to the slow detector used in experiment.

The underlying physical mechanism for SC generation are the modulation instability (MI), which plays an important role in the initial stage of SC generation, and the soliton self-frequency shifted Raman scattering, which leads to a SC spectrum shift toward the long-wavelength side [21]. The symmetrical MI side bands can be seen on both spectral sides in (Fig. 2b) when the SC output power was 1.97 W, and the sidebands were separated by ~13, ~26 and ~39 nm from the pump laser at 2054 nm. The frequency shift of MI gain peaks from the pump laser can be calculated by $\Delta\nu_n = n(2\gamma P_0/|\beta_2|)^{1/2}/2\pi$ ($n = \pm1, 2, 3, ...$), where γ is the nonlinearity coefficient, P_0 is the pump peak power and β_2 is the group velocity dispersion parameter of the fibre at the pump wavelength. When the output SC power is 1.97 W, the estimated pump peak power P_0 is 12.61 kW. Then at $\gamma = 8\times10^{-2}$ W^{-1} km^{-1} and β_2 = –56 ps^2 km^{-1}, and the calculated frequency shift $\Delta\nu_n = 0.955n$ (THz) and $\Delta\lambda_n = 13.5n$ (nm), which is close to the experimentally observed value.

At a maximal pump power, the spectral evolutions of the SC laser were studied for different MMF length (Fig. 3). As the MMF length is cut back from 30 m down to 15 m, the long-wavelength edge of the SC increases from ~2500 nm to ~2600 nm along with an increase in the overall spectral density. One can see that the reason responsible for the wide spectrum generation is the nonlinear processes occurring

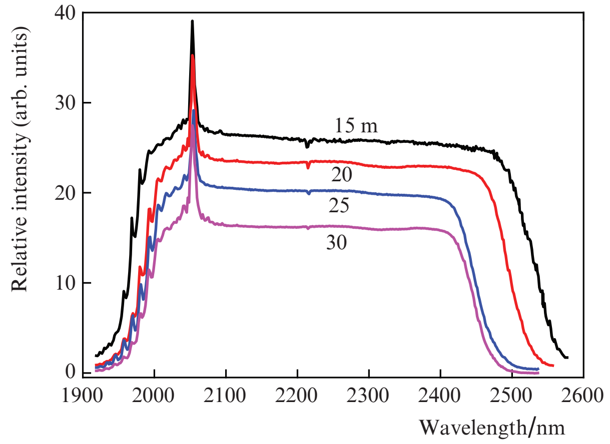

Figure 3. Evolution of the SC spectrum for different MMF lengths.

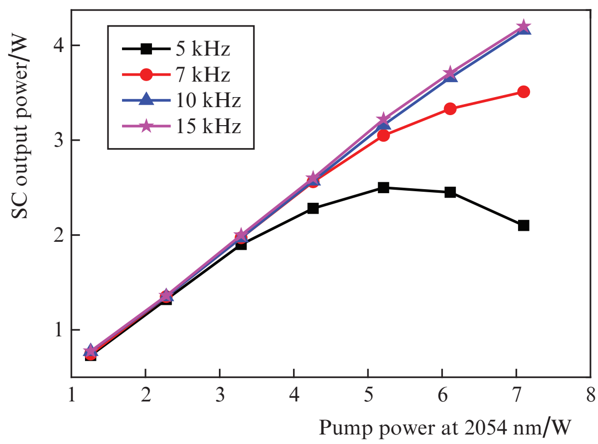

Figure 5. Output SC power vs. pump power in MMF at different PRFs.

within the first few meters of the MMF, and propagation through longer distances merely attenuates the spectrum due to the high loss associated with the silica glass absorption beyond 2.4 μm. Thus, obtaining the broadest spectrum requires the appropriate fibre length where nonlinearity dominates over loss.

The average output SC power was measured by a powermeter (Coherent, PM30) with a thermal sensor response range of 0.15–11 μm, covering the entire SC spectral band. The average output SC power as a function of pump power is shown in Fig. 4. As can be seen, the maximal obtained SC output powers in SMF and MMF, including the peak at 2054 nm, were 0.53 W and 3.51 W at 7 kHz, and the corresponding optic-to-optic conversion efficiencies were 34.6% and 73.7% with allowance fot the coupling efficiency. The maximal achieved pulse energies of SC (E_P) were 75.7 μJ and 500 μJ in SMF and MMF. It also can be seen when the pump power is greater than 5.21 W in MMF, the output SC power begins to saturate, and a further increase in the pump power does not lead to a linearly increase in the SC output power. We attribute the SC power saturation to the power loss of the SC long-wavelength edge (> 2.4 μm) in MMF, caused by the multiphonon absorption in silica fibre.

Figure 5 shows the output SC power at different PRFs. As can be noticed, for pump power of 7.1W, the obtained output SC power increased from 2.1 to 4.2 W by increasing the PRF from 5 to 15 kHz, and the corresponding optic-to-optic conversion efficiency increased from 44.1% to 88.2%.

A fast InGaAs photodiode and a 350 MHz digital oscilloscope (Wavejet 332, Lecroy) were used to measure the time-domain SC pulse duration. Typical temporal profiles of the SC pulses at a maximum output power are shown in Fig. 6. Compared to the pump pulse, the SC pulse shapes are somewhat distortion: the SC pulse shapes are not broken up into a series of short pulses, so that the SC energies are still concentrated in one pulse. One can see that the full-width at half maximum (FWHM) of SC pulse duration (t_{sc}) SMF is ~42.1 ns (compared to a 29 ns pump pulse). For MMF, the t_{sc} is approximately ~35.7 ns (compared to 25 ns pump pulse). We attribute the main reason to the MI effect which was involved

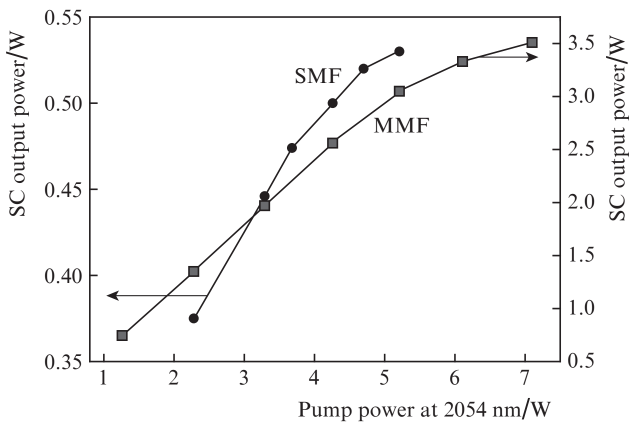

Figure 4. Output SC power vs. pump power for SMF and MMF.

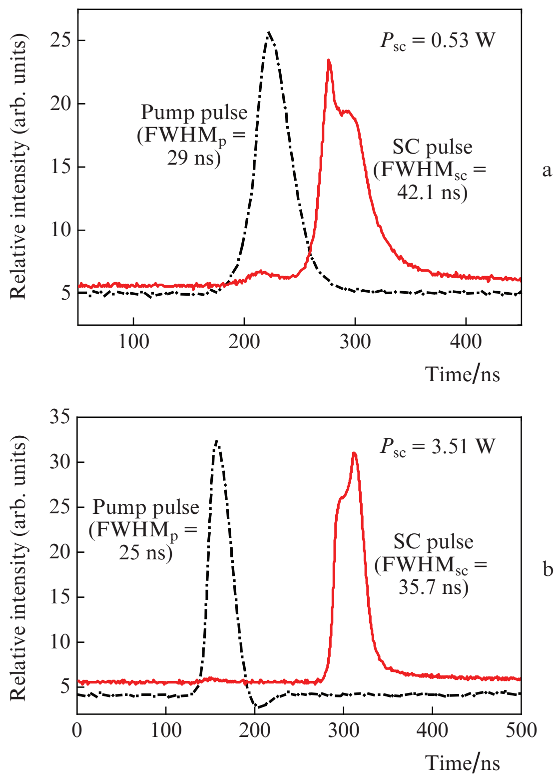

Figure 6. Output SC pulse shape for SMF and MMF.

in the SC generation and could overmodulate the output pulse with signatures of pulse splitting.

The peak SC power can be estimated as $P_{sc} = E_{sc}/t_{sc}$ with $P_{sc} \approx 1.8$ and 14 kW for SMF and MMF, respectively.

The monitored stability of the output SC power in SMF and MMF revealed the presence of significant variations in the SC output power in SMF, the main reason of which is the fact that the SMF core is small, and the coupling efficiency of the pump power is easily influenced by the environment factor. Figure 7 shows the fluctuation of the SC power in MMF within a week. As can be, the maximal fluctuation of the output power was 0.2 W with the fluctuation proportion of less than 6%. The beam quality of the SC spectrum in MMF was also evaluated. The SC light separated by a dichromatic mirror ($R \geqslant$ 90% at ~2.1 μm) was focused by an $f = 150$ mm coated lens, and the intensity profile of the laser beam was mapped at difference axial locations around the focal spot by using a 90/10 knife edge cutting across the beam. The M^2 value was estimated by fitting the beam shape to the Gaussian beam propagation profile, and the estimated values was 1.15 at 3.51 W (see the inset in Fig. 7).

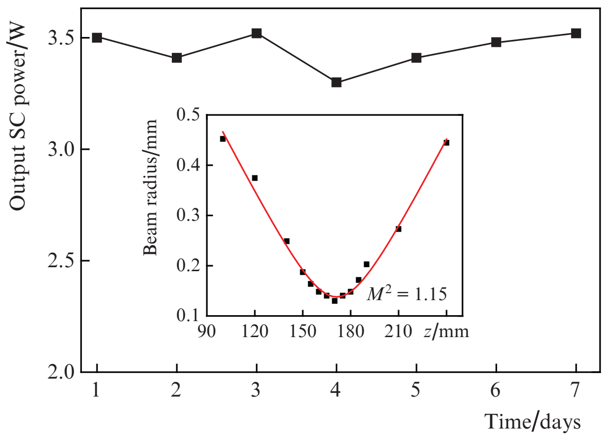

Figure 7. Fluctuation of the output SC power in seven days. The centre wavelength is 2.1 μm.

4. Conclusions

A broadband SC laser based on telecommunication fibre directly pumped by a nanosecond Q-switched Tm, Ho : YVO_4 laser is reported. An overall output SC power of up to 0.53 W in the band of ~1950 nm to 2500 nm from 15-m-long SMF is obtained, and the SC spectrum is characterised by a high flat spectrum distribution of the intensity (< 2%) in the wavelength interval of 2070–2390 nm. Pumping the same length MMF it is possible to achieve 3.51 W of output power in the ~1900–2600 nm spectral band, and the SC spectrum has an extremely high flat profile with negligible intensity variation in the band of 2070–2475 nm. The time-domain SC pulses are measured, and no split is found. The SC output power is stable with < 6% fluctuation in MMF. Due to the high absorption of silica fibre in > 2.4 μm region, the output SC spectrum and average power are limited by the MMF length. In the future, we will couple the 2 μm pump to low mid-IR loss fibre such as ZBLAN fluoride fibre, due to which the output SC spectrum can be extended toward longer wavelength.

References

1. Powers M.A., Davis C.C. *Appl. Opt.*, **51**, 1468 (2012).
2. Sych Y., Engelbrecht R., Schmauss B., Kozlov D., Seeger T., Leipertz A. *Opt. Express*, **18**, 22762 (2010).
3. Waynant R.W., Ilev I.K., Gannot I. *Phil. Trans. R. Soc. Lond. A*, **359**, 635 (2001).
4. Buczynski R., Pysz D., Martynkien T., Lorenc D., Kujawa I., Nasilowski T., Berghmans F., Thienpont H., Stepien R. *Laser Phys. Lett.*, **6**, 575 (2009).
5. Lehtonen M., Genty G., Ludvigsen H., Kaivola M. *Appl. Phys. Lett.*, **82**, 2197 (2003).
6. Lin J.H., Lin K.H., Hsu C.C., Yang W.H., Hsieh W.F. *Laser Phys. Lett.*, **4**, 413 (2007).
7. Brambilla G., Koizumi F., Finazzi V., Richardson D.J. *Electron. Lett.*, **41**, 795 (2005).
8. Moghaddam M.R.A., Harun S.W., Akbari R., Ahmad H. *Laser Phys. Lett.*, **8**, 369 (2011).
9. Abeeluck A.K., Headley C., Jorgensen C.G. *Opt. Lett.*, **29**, 2163 (2004).
10. Liao M.S., Yan X., Qin G.S., Chaudhari C., Suzuki T., Ohishi Y. *Opt. Express*, **17**, 15481 (2009).
11. Swiderski J., Michalska M., Kieleck C., Eichhorn M., Maz G. *IEEE J. Photon Tech. Lett.*, **26**, 150 (2014).
12. Kulkarni O.P., Alexander V.V., Kumar M., Freeman M.J., Islam M.N., Terry F.L., Neelakandan M., Chan A. *J. Opt. Soc. Am. B.*, **28**, 2486 (2011).
13. Qin G., Yan X., Kito C., Liao M., Chaudhari C., Suzuki T., Ohishi Y. *Appl. Phys. Lett.*, **95**, 161103 (2009).
14. El Amraoui M., Gadret G., Jules J.C., Fatome J., Fortier C., Désévédavy F., Skripatchev I., Messaddeq Y., Troles J., Brilland L., Gao W., Suzuki T., Ohishi Y., Smektala F. *Opt. Express*, **18**, 26655 (2010).
15. Alexander V.V., Shi Z.N., Islam M.N., Ke K., Freeman M.J., Ifarraguerri A., Meola J., Absi A., Leonard J., Zadnik J., Szalkowski S.A., Boer G.J. *Opt. Lett.*, **38**, 13 (2013).
16. Kurkov A.S., Kamynin V.A., Tsvetkov V.B., Sadovnikova Ya.E., Marakulin A.V., Minashina L.A. *Kvantovaya Elektron.*, **42**, 778 (2012) [*Quantum Electron.*, **42**, 778 (2012)].
17. Kamynin V.A., Kurkov A.S., Mashinsky V.M. *Laser Phys. Lett.*, **9**, 219 (2012).
18. Swiderski J., Maciejewska M. *Appl. Phys. B*, **12**, 513-1 (2012).
19. Kurkov A.S., Sholokhov E.M., Sadovnikova Y.E. *Laser Phys. Lett.*, **8**, 598 (2011).
20. Kamynin V.A., Kurkov A.S., Tsvetkov V.B. *Kvantovaya Elektron.*, **41**, 986 (2011) [*Quantum Electron.*, **41**, 986 (2011)].
21. Xia C.N., Kumar M., Cheng M.Y., Kulkarni O.P., Islam M.N., Galvanauskas A., Terry F.L., Freeman M.J., Nolan D.A., Wood W.A. *IEEE J. Sel. Top. Quantum Electron.*, **13**, 789 (2007).